RSC Applied Polymers

ROYAL SOCIETY OF CHEMISTRY

COMMUNICATION

View Article Online
View Journal | View Issue

Cite this: *RSC Appl. Polym.*, 2026, **4**, 524

Received 15th November 2025,
Accepted 23rd January 2026

DOI: 10.1039/d5lp00359h

rsc.li/rscapplpolym

Ionogel thin films as a compatibilizing pretreatment for electrospray deposition

Tejasvi Venkat,[a] Hannah Mow,[b] Emily Li,[c] Weronika Wasniowska,[d] Ayman Rouf,[b] Noah M. McAllister,[b] Zainab Al-Jaleel[b] and Jonathan P. Singer *[a,b,d]

Electrospray deposition applies thin films to conductive or hydrated targets, but not insulators, due to charge repulsion. Pretreatment of coating insulating substrates with the use of removable ionogel thin films 100–800 nm produces (self-limiting) electrospray deposition coatings of similar thicknesses to those produced on conductive surfaces, independent of humidity.

Introduction

Electrospray deposition (ESD) has become a well-established technique in the last six decades since Blumberg *et al.*'s first report.[1] Despite this, the technology has been primarily utilized as a characterization tool, while the related techniques of electrospinning and electrostatic spray have found widespread industrial applications.[2–6] In ESD, a flowing solvent placed under a strong electric field is atomized, depositing its solute on a grounded target. ESD exhibits several advantages for manufacturing, including the creation of mono- or bi-disperse[7–11] droplet sprays and the non-inertial nature of the technique, leading to limited overspray. For these and other reasons, ESD was revisited as a manufacturing technique in the past few decades and has been frequently shown in bench studies as a tool for the creation of thin films and particles. More recently, ESD has been demonstrated as a powerful tool for coating complex 3D surfaces. Our research has demonstrated that operating in the self-limiting electrospray deposition (SLED)[12] regime makes ESD compatible with the conformal coating of cm-scale 3D objects and even reentrant features, including apertures as small as 50 μm.[13] SLED coatings are always formed of particles because of the requirement for low mass transport mobility in the deposit to build up charge; however, the porous coatings can be densified by either thermal or solvent vapor annealing for either measurement or final applications.[12,14] Through SLED, complex structures can be coated with hollow shell, nanowire, and composite[15] particulate coatings that can add surface functionality, such as wetting manipulation,[13,16] plasmonic color,[15] bioactivity,[17] or conductive/catalytic surfaces.[18] Having demonstrated this capability, it becomes of greater interest to expand its applicability, and that of ESD in general, to as many potential targets as possible, ideally, through some facile preprocess of adding a "compatibilization layer" that dissipates surface charge. In addition, having the means to remove the compatibilization layer under mild conditions and with minimal residue would eliminate any potential effects of the treatment on the final properties.

To date, there has been limited thought given to the importance of substrate conductivity in ESD beyond the binary insulator *versus* conductor. That said, the problem of placing conductive coatings on insulating surfaces is of great interest. This is a common issue in electroplating, where the metallization of, for example, polymers is possible, but typically requires the application of a thin layer of conductive material, such as electroless silver/nickel or a colloidal paint. The requisite charge transport for ESD processes is much less than that for electroplating, as evidenced by the use of the related electrostatic spray technique in the coating of plants with pesticides. In such systems, the hydrated, ion-rich surface of the plant is sufficient to dissipate the charge. This is because the charge flux of ESD is much less than that of electroplating (~1 μA cm^{-2} *versus* ~1 mA cm^{-2}). Our previous results have confirmed similarly that SLED sprays can coat hydrogel materials (provided that the hydrogel is infused with ionized water)[13] or plants.[15] Furthermore, we and others have observed that borosilicate glass can be sprayed with a thin ESD coating in humid environments.[19–21] Indeed, without humidity, glass targets rapidly destabilize sprays on the order of seconds.[20] Most recently, it has been reported that soaking hydrophilic polymer structures in water or exposing them to high humidity (>40%) can increase their compatibility with spray in a similar

[a]*Department of Materials Science and Engineering, Rutgers, The State University of New Jersey, Piscataway, NJ 08854, USA. E-mail: jonathan.singer@rutgers.edu*
[b]*Department of Mechanical and Aerospace Engineering, Rutgers, The State University of New Jersey, Piscataway, NJ 08854, USA*
[c]*Department of Electrical and Computer Engineering, Rutgers, The State University of New Jersey, Piscataway, NJ 08854, USA*
[d]*Department of Biomedical Engineering, Rutgers, The State University of New Jersey, Piscataway, NJ 08854, USA*

fashion.[22] As will be discussed, this is not possible with fused quartz or sapphire, indicating that this dissipation mechanism relies on a combination of surface absorbed water and ionic dopants. This is consistent with the universal increase in surface conductivity and capacitance[22] with absorbed humidity and its increased significance on hydrophilic or polarizable surfaces.[23–25] These results suggest that compatibilizing insulating surfaces for ESD (and SLED) may be achievable using much thinner coatings of conductive material than required for electrodeposition or even through the use of hydrophilic layers. The potential benefit of having such a preprocess is the application of ESD and SLED to both high-end industries that demand ceramic or plastic substrates, such as nanoparticle coatings on optics or semiconductor packaging, or to commodity products that demand cheap materials and processes, such as the electrostatic painting of injection-molded or additively manufactured plastics for aesthetic purposes.

Here, we show that thin films of an ionogel can serve as a more universal approach at sub-micron thicknesses and at any humidity (Fig. 1b). The ionogel we used is formed of the ethyl

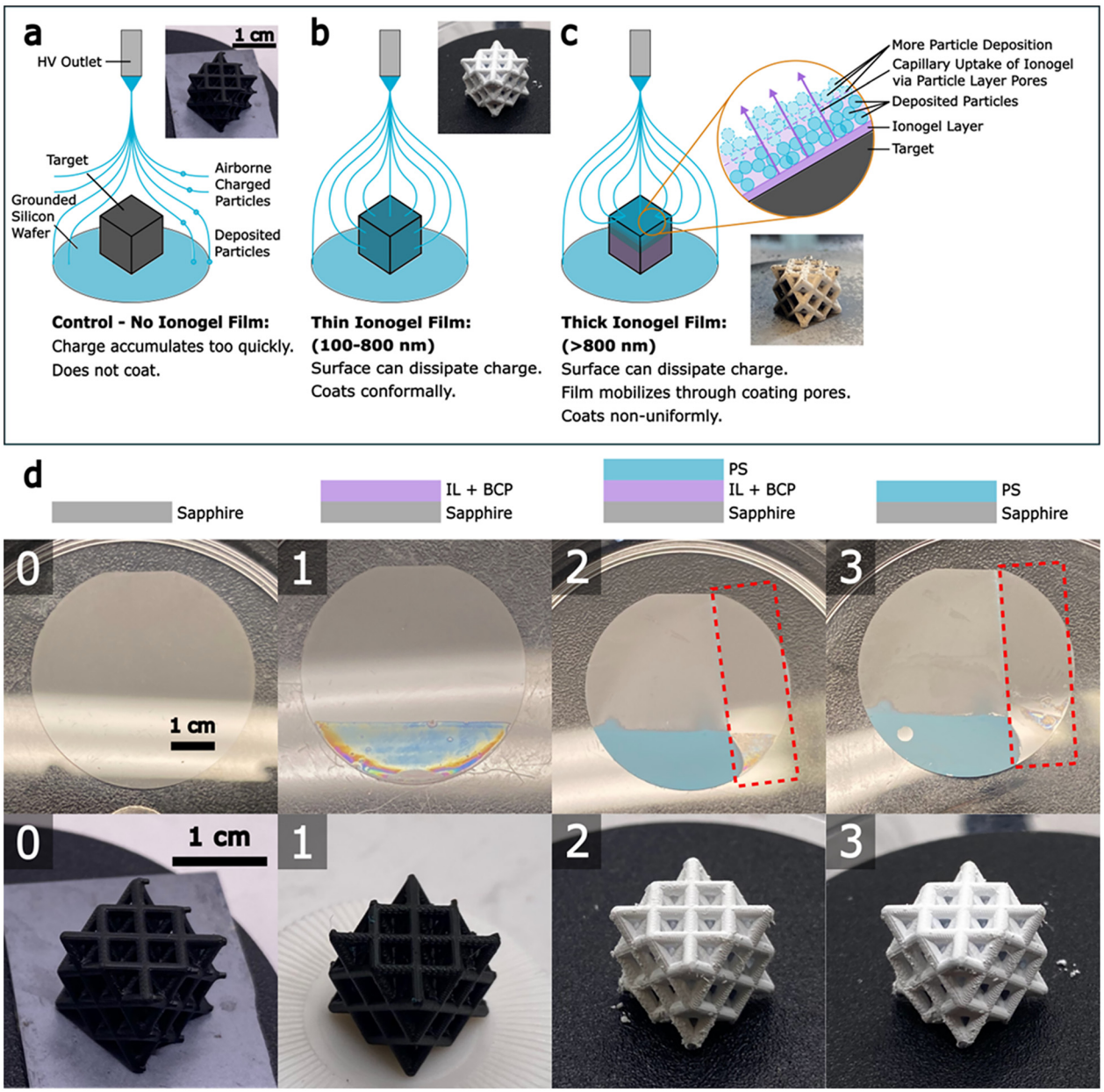

Fig. 1 Top: Schematic of SLED with (a) an unaltered insulating substrate, (b) a sub-micron thick ionogel film, and (c) a thicker film. (d) Bottom: Step-by-step treatment process from (0) an unaltered substrate to (1) dip-coated with an ionogel thin film to (2) electrosprayed with a porous PS coating (+ trace Oil Blue dye for sapphire) to (3) ethanol-rinsed with the porous PS coating only, the ionogel removed, on a sapphire wafer and a urethane lattice. The inset of the sapphire results shows a schematic of the added layers and the dotted red box indicates the position of the grounding carbon tape. Lattices sprayed in a dry chamber (RH = 18%–20%).

ammonium nitrate (EAN) ionic liquid (IL) and the Pluronic F127 poloxamer block copolymer (BCP), as previously reported by López-Barrón *et al.*[26] We chose this gel as it forms an immobilized, electrically conductive thin film that does not rely on absorbed water and can be readily dip-coated or printed without plasma treatment.

Materials and methods

Polystyrene (molecular weight = 35 kDa, Sigma Aldrich), Pluronic F127 (PEO106–PPO70–PEO106) (molecular weight = 12.6 kDa, Sigma Aldrich), Oil Red EGN (>90%, Sigma Aldrich), Oil Blue 35 (>96%, Sigma Aldrich), ethyl ammonium nitrate (>97%, IoLiTec), and 2-butanone (>99%, Sigma Aldrich) were used as received. Sapphire disks and silicon wafers were sourced from various suppliers. Urethane additive-manufactured lattices were provided by Carbon Inc., and thermoplastic resin injection molded figurines (Reaper Miniatures – Bones USA) were used as purchased.

A typical procedure is shown in Fig. 1d. To investigate the effect of the ionogel film (or "film") thickness on the SLED coating (or "coating") thickness, multiple concentrations of 70 : 30 ratios of EAN IL to Pluronic F127 BCP by weight in DI water were prepared. The IL : BCP ratio was selected to be confidently in the gel state, as reported in the literature.[26] Dip coating was performed at various deposition rates on a home-built apparatus designed around a Newport IMS500CC linear stage. After dipping, the samples were dried at room temperature overnight and used within 7 days to prevent effects of ambient humidity. ESD was performed using a KD Scientific syringe pump and a Gamma High Voltage Research ES30P-5W/DAM power supply. The dipped samples were placed on a silicon wafer on a metal grounding plate and connected from the dipped surface to the wafer with conductive carbon tape. Spraying was then conducted with 1 wt% PS solutions in MEK with trace Oil Red dye at 0.5 mL h^{-1} for 60 minutes on flat samples and, for 3D samples, at 0.3 mL h^{-1} until fully coated as specified.

Ionogel coatings were measured directly on sapphire substrates with a microscopic reflectometer (Filmetrics F40EX) connected to a motorized stage (Zaber E13F33E) using custom Python software as described previously.[12] Automated mapping was not possible due to the low reflectivity contrast, which required manual tuning of the wavelength sampling range at each point. Eight points were selected in disparate regions, as shown in Fig. 2a, of the ionogel films to obtain average gel thicknesses. Lattices were sprayed in a dry chamber (RH = 18%–20%) and all other samples were sprayed in ambient humidity (RH = 40%–60%). After spraying, the PS thickness was measured using contact profilometry (Bruker DektakXT-A) of the films after ethanol rinse for 20–40 seconds and acetone vapor smoothing.

Fourier transform infrared spectroscopy was performed with a Nicolet iS20 FTIR spectrometer in the attenuated total reflectance (ATR) mode. Optical microscopy images were taken with a Leica DM2700 in the reflection mode.

Results and discussion

Before arriving at the ionogel treatment, we conducted a preliminary investigation to determine if hydrophilic polymers, when combined with elevated humidity, could serve as an appropriate pretreatment for ESD, and, most relevant to 3D applications, conformal SLED. The key results are summarized in the SI. These conclude that coatings on the order of single microns would be needed, and further that these pretreat-

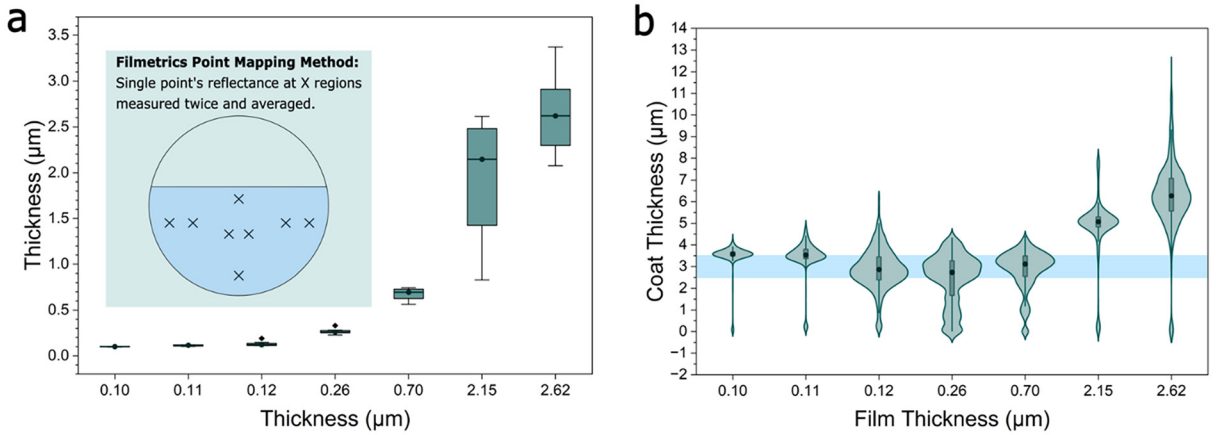

Fig. 2 (a) (inset) Mapping method used to obtain the average film thickness of a sample with optical reflectometry. Film thickness box plot distribution for each sample, with the median marked by a dot and line. The average film thickness obtained from these measurements is used as a sample label for the *x*-axes for (a and b), but are not to scale. Details for each sample can be found in the SI. (b) PS coat contact profilometry thickness violin plot distribution for each sample, with the median marked by a dark dot. Sub-micron thick films coat within an expected SLED thickness range of PS deposited on silicon (2.5–3.5 microns, highlighted in blue). F-G samples of thicker films exceed the expected SLED thickness. It should be noted that some of the low thickness values represent the onset of the film in the profilometer (see Fig. S3).

ments would necessitate humidity levels >40% to allow for sufficient charge dissipation. In addition, these coatings often required plasma pretreatment of the targets, which can limit 3D complexity.

In contrast, ionogel coatings enabled ESD at any measurable thickness, and coatings down to 100 nm could be readily obtained on sapphire disks, with thinner coatings resulting in dewetting. We believe that the cohesion of the films, even in the absence of plasma treatment, was due to the entangled triblock copolymer structure of the poloxamer ionogel, as evidenced by a characteristic terraced pattern[27] corresponding to ~10 nm swollen triblock steps. These steps were so uniform that they could be readily observed in optical microscopy (Fig. S2). In the SLED regime, uniform thicknesses consistent with the results on silicon wafers were observed for submicron ionogel films (Fig. 2b). However, non-uniform, thick coatings were obtained when the dipped ionogel was too thick (>800 nm). In this figure, a violin plot is used for each profile to disambiguate the onset of the profile, which contains both thicker and thinner values for a given profile as can be seen in the detailed contact profilometry of each case in Fig. S3. The central mass of the plot is the dominant coating behavior, and its width demonstrates both roughness and thickness variation. In the thicker cases, it was also observed that the SLED would overspray the dipped region (Fig. S3) and that the porous SLED coatings would become transparent over time (Fig. S4a and b) but could be reverted to scattering through a short ethanol rinse (Fig. S4c and Video S1). This suggests that the origin of the breakdown of the SLED effect is the capillary uptake of the IL into the coating (Fig. 1c). Thinner ionogel coatings either do a better job of retaining their IL or do not contain enough IL to create a conductive pathway in a microscale coating. This behavior is also observed when moving to 3D structures. Fig. S5a–c show a series of thermoplastic figur-

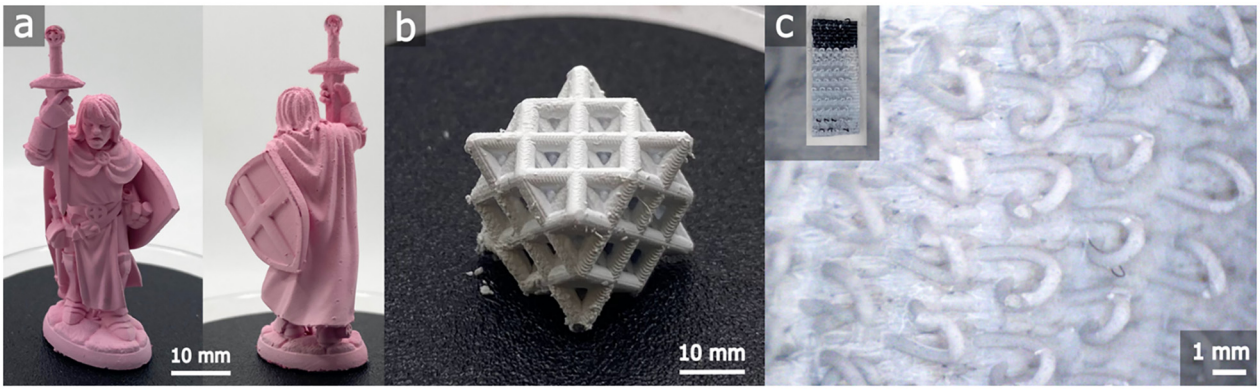

Fig. 3 (a) Thermoplastic figurine, (b) urethane lattice, and (c) nylon Velcro hooks dipped in 3.3 wt% ionogel solution and electrosprayed with 1% PS in MEK (+ trace Oil Red dye for (a)).

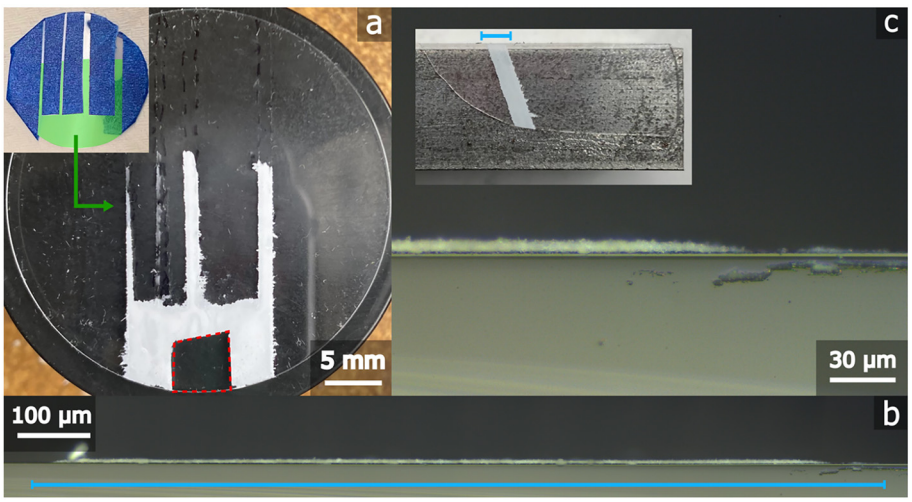

Fig. 4 (a) Coated target region (shown in the green inset) painted onto a sapphire wafer with 0.825 wt% ionogel solution, sprayed with 1% PS in MEK at 0.5 mL h^{-1} for 60 minutes, and ethanol-rinsed for 30 seconds. The dotted red box indicates the position of the grounding carbon tape. Note that the second line from the left dewetted during film formation. (b) Stitched cross-section of the line pictured in the (c) inset showing the sapphire-particle interface under dark field optical microscopy using a 20× objective. (c) 50× objective image of the transitional zone of (b).

ines dipped at progressively lower concentrations of the ionogel until a dipping concentration of 3.3% in water is reached. Notably, this concentration is too low to give a continuous film on an atomically smooth flat surface (*i.e.*, sapphire), but on rougher polymeric 3D substrates, this coating appears to provide a robust pathway to conformal coatings, even on complex additively manufactured or injection molded structures (Fig. 3). This is consistent with roughness leading to higher liquid film stability and thickness in dip coating.[28] It should be noted that not every substrate attempted could be coated in this way, indicating that roughness is not the only factor. Indeed, while some polymeric surfaces, including the 3D structures and ethylene shrink wrap (Fig. S6), could be coated, smooth and highly hydrophobic polymer surfaces (*e.g.*, Kapton polyimide or Sylgard 184 silicone) still resulted in film dewetting; however, this could potentially be addressed in future work through the use of non-aqueous dipping solution, plasma/ozone treatment, or deliberate surface roughening.

Another advantage of this approach over using hydrated hydrophilic surfaces is its capability for selective patterning. A sufficiently thin, continuous ionogel film formed on an insulating surface allows for selective deposition onto regions of the film. This ability is demonstrated with hand-painted lines out of a blocked region for easy grounding using a masking tape approach (Fig. 4). Coating conformal to the design path is observed, and cross-sectional views show uniform coating throughout the midregion of the pattern with a small ~30 μm transitional zone at the edges (Fig. 4b and c). Furthermore, numerous means exist for precision writing, such as inkjet or screen printing, and our prior work has demonstrated that SLED can be applied to sub-100 μm features and feature spacings without overlap.[18,29]

Lastly, for a given application, it may be desirable to remove the template layer, or at least the semi-mobile IL component. As shown in Fig. S4, a short ethanol rinse can be employed to this effect; however, in situations where solvent is undesirable, the EAN IL can also be readily evaporated well below its reported boiling point, as confirmed by FTIR (Fig. S7). This showed that the IL was undetectable after 1 h of baking at 75 °C, making it compatible with a wide range of materials.

Conclusion

With the use of an ionogel composed of EAN and Pluronic F127, we can create sub-micron coatings that enable ESD (and SLED) on nonconductive substrates *via* dip coating or direct writing. The IL can be removed either thermally or together with the BCP *via* solvent dipping. This has numerous advantages over hydrated thin films as a pretreatment, with the caveat that the applied films cannot be too thick (here, >800 nm). Thicker coatings allow the IL to drain from the pretreatment into the applied coating, allowing for additional SLED. It should be noted that this report only considered a single ionogel, and there are numerous other IL–polymer combinations that can be explored to eliminate this restriction; however, even with the capabilities shown, this pretreatment approach greatly expands the potential selection of substrates and templates for SLED, enabling future applications in, for example, applying functional coatings to economical surfaces created by polymer injection molding or additive manufacturing. While not considered in this initial report, the adhesion of both porous and densified SLED coatings will need to be evaluated on whatever surface is the deposition target for a given application.

Conflicts of interest

J. P. S. is the inventor/coinventor of several patents and applications on SLED. No other author has conflicts to declare.

Data availability

The data supporting this article have been included as part of the supplementary information (SI). Supplementary information is available, including a preliminary study on hydrophilic coatings in high ambient humidity, optical microscopy, additional profilometry data, images and video of removal of absorbed ionic liquid, additional ionogel pretreatment results, and FTIR spectroscopy showing thermal and solvent removal of the pretreatment. See DOI: https://doi.org/10.1039/d5lp00359h.

Acknowledgements

This work was funded by the NSF through CMMI Awards 1911518, 2019849, and 2335614. T. V. and A. R. acknowledge support from the Rutgers Aresty Program. N. M. M. and H. M. acknowledge support from the New Jersey Space Grant Consortium, funded by NASA, through the student fellow program. We thank Carbon Inc. for providing printed lattices. The authors also acknowledge the New Jersey Advanced Manufacturing Institute for the use of the FTIR spectrometer.

References

1 L. N. Blumberg, J. C. Gursky and P. C. Stein, *Electrospraying of Thin Targets*, Los Alamos Scientific Laboratory, 1962.
2 S. S. Bhagure and A. R. Rao, *Int. J. Innov. Sci. Res. Technol.*, 2020, **5**, 528–538.
3 S. E. Law, *J. Electrost.*, 2001, **51**, 25–42.
4 J.-S. Park, *Adv. Nat. Sci.: Nanosci. Nanotechnol.*, 2011, **1**, 043002.
5 L. Persano, A. Camposeo, C. Tekmen and D. Pisignano, *Macromol. Mater. Eng.*, 2013, **298**, 504–520.
6 P. Vass, E. Szabó, A. Domokos, E. Hirsch, D. Galata, B. Farkas, B. Démuth, S. K. Andersen, T. Vigh and G. Verreck, *Wiley Interdiscip. Rev.: Nanomed. Nanobiotechnol.*, 2020, **12**, e1611.
7 B. Almería and A. Gomez, *J. Colloid Interface Sci.*, 2014, **417**, 121–130.

8 A. Gomez and W. Deng, *Aerosol Meas.*, 2011, 435–448.
9 S. Kavadiya and P. Biswas, *J. Aerosol Sci.*, 2018, **125**, 182–207.
10 S. K. Boda, X. Li and J. Xie, *J. Aerosol Sci.*, 2018, **125**, 164–181.
11 O. Wilhelm, L. Mädler and S. E. Pratsinis, *J. Aerosol Sci.*, 2003, **34**, 815–836.
12 L. Lei, D. A. Kovacevich, M. P. Nitzsche, J. Ryu, K. Al-Marzoki, G. Rodriguez, L. C. Klein, A. Jitianu and J. P. Singer, *ACS Appl. Mater. Interfaces*, 2018, **10**, 11175–11188.
13 D. A. Kovacevich, L. Lei, D. Han, C. Kuznetsova, S. E. Kooi, H. Lee and J. P. Singer, *ACS Appl. Mater. Interfaces*, 2020, **12**, 20901–20911.
14 N. M. McAllister, R. A. Green-Warren, M. Arkhipov, J.-H. Lee, A. A. Pelegri and J. P. Singer, *Eng. Rep.*, 2024, **6**, e12830.
15 L. Lei, S. Chen, C. J. Nachtigal, T. F. Moy, X. Yong and J. P. Singer, *Mater. Horiz.*, 2020, **7**, 2643–2650.
16 C. J. Nachtigal, Y. Li, L. Zhang, L. Lei, M. D. Losego and J. P. Singer, *Adv. Eng. Mater.*, 2022, **24**, 2101485.
17 S. H. Park, I. R. Shah, N. C. Jhumur, Y. Mo, S. Tendolkar, E. O. Lallow, J. W. Shan, J. D. Zahn, J. N. Maslow, A. A. Pelegri, H. Lin, D. I. Shreiber and J. P. Singer, *Soft Matter*, 2025, **21**, 3207–3214.
18 M. J. Grzenda, J. Yu, M. Atzampou, C. E. Shuck, Y. Gogotsi, J. D. Zahn and J. P. Singer, *Small*, 2024, e2405509, DOI: 10.1002/smll.202405509.
19 N. A. Brown, Y. Zhu, G. K. German, X. Yong and P. R. Chiarot, *J. Electrost.*, 2017, **90**, 67–73.
20 Y. Zhu and P. R. Chiarot, *J. Phys. D: Appl. Phys.*, 2020, **54**, 075301.
21 H. Hu, K. Toth, M. Kim, P. Gopalan and C. O. Osuji, *MRS Commun.*, 2015, **5**, 235–242.
22 E. E. Pawliczak and P. R. Chiarot, *SSRN*, 2025, preprint, DOI: 10.2139/ssrn.5564668.
23 G. Sawa and J. H. Calderwood, *J. Phys. C:Solid State Phys.*, 1971, **4**, 2313.
24 Y. Awakuni and J. H. Calderwood, *J. Phys. D: Appl. Phys.*, 1972, **5**, 1038.
25 V. T. C. Paiva, L. P. Santos, D. S. da Silva, T. A. L. Burgo and F. Galembeck, *Langmuir*, 2019, **35**, 7703–7712.
26 C. R. López-Barrón, R. Chen, N. J. Wagner and P. J. Beltramo, *Macromolecules*, 2016, **49**, 5179–5189.
27 K. Fukunaga, H. Elbs, R. Magerle and G. Krausch, *Macromolecules*, 2000, **33**, 947–953.
28 R. Krechetnikov and G. M. Homsy, *Phys. Fluids*, 2005, **17**, 102108.
29 M. J. Grzenda, M. Atzampou, A. Samateh, A. Jitianu, J. D. Zahn and J. P. Singer, *Coatings*, 2023, **13**, 599.